J. Fluid Mech. (1987), *vol.* 176, *pp.* 117–134
Printed in Great Britain

Numerical and experimental study of the transformation of a solitary wave over a shelf or isolated obstacle

By FERNANDO J. SEABRA-SANTOS†, DOMINIQUE P. RENOUARD AND ANDRÉ M. TEMPERVILLE

Institut de Mécanique de Grenoble, B.P. 68, 38402 Saint-Martin d'Hères Cedex, France

(Received 5 July 1985)

In order to model the evolution of a solitary wave near an obstacle or over an uneven bottom, the long-wave equations including curvature effects are introduced to describe the deformation and fission of a barotropic solitary wave passing over a shelf or an obstacle. The numerical results obtained from these equations are shown to be in good agreement with an analytical model derived by Germain (1984) in the framework of a generalized shallow-water theory, and with experimental results collected in a large channel equipped with a wave generator. Given the initial conditions, i.e. amplitude of the incident solitary wave, water depth in the deep region, and height of the shelf or the barrier, it is possible to predict the amplitude and number of the transmitted solitary waves as well as the amplitude of the reflected wave, and to describe the shape of the free surface at any time.

1. Introduction

The reflection of solitary waves from a plane, vertical wall has been studied both analytically and numerically (Su & Mirie 1980; Mirie & Su 1982; Fenton & Rienecker 1982) and experimentally (Maxworthy 1976). In a previous paper (Renouard, Seabra-Santos & Temperville 1985) we proposed both an analytical study, within the framework of shallow-water theory, and a numerical solution of a KdV equation modified to take account of viscous effects. We compared the analytical and numerical results thus obtained with experimental data. Agreement was found to be remarkably good between the number and amplitude of solitary waves generated by a paddle movement, and the propagation and damping of such waves, but some slight differences appeared in the neighbourhood of the wall when we analysed the reflection of a solitary wave from a plane, vertical wall. As in Maxworthy (1976), we were led to think that, locally, the characteristics of the fluid motion near the wall no longer fulfilled the conditions of the theory. The numerical resolution of Serre's equation (Seabra-Santos 1985) appeared to provide a way to overcome this difficulty, and will be generalized here to describe the phenomena occurring when an incident solitary wave passes over a shelf or an immersed obstacle. These numerical results will be compared with experiments. One of the most striking effects of the passage of a single solitary wave over a step is its fission into two or more solitary waves. This phenomenon can be described analytically (Germain 1984), and the number and amplitude of the solitary waves resulting from the fission of the incident solitary wave

† Permanent affiliation: Faculdade de Ciencias e Tecnologia Universidade de Coimbra, Portugal.

as well as the amplitude of the reflected solitary wave can be predicted and compared with the experimental data.

The first study of the consequences of the passage of a solitary wave above a bottom slope is probably that of McCowan (1894), who was only interested in wave breaking. The first report clearly indicating the fission of such a wave over a shelf was given by Street, Burges & Whitford (1968). Madsen & Mei (1969) used approximate equations for long waves over an uneven bottom and the method of characteristics to show the disintegration of the incident wave into a train of solitary waves of decreasing amplitude, and they provided experimental data to support their conclusions. Unfortunately their experimental facility did not allow them to observe the final stage of fission, and they gave no indication of a reflected wave. A more comprehensive study was provided by Goring (1978), using a much larger facility, which compared experimental results with three different models, namely a linear non-dispersive, a nonlinear dispersive and a linear dispersive theory. He showed that the nonlinear dispersive theory compared favourably with the experiments in the height, shape and propagation of the reflected solitary wave. Though mentioning the splitting of the single incident wave into a number of solitary waves over the shelf, in his conclusions Goring (1978) only mentioned (*a*) the nonlinear dispersive theory and also a description of wave propagation over the slope, and (*b*) the distinction between the distance for the dispersive effects to become important, and the distance for the nonlinear effects to become important. Regarding the disintegration of the incident wave, he computed the number and amplitude of the transmitted waves by the inverse scattering method, using the shape of the free surface near the step as initial data. The purpose of the present study is to provide another approach to this phenomenon, supported by numerous and precise experimental data.

We shall introduce modified long-wave equations which take into account strong curvature effects, a generalization of the Serre (1953) equations for a channel with variable depth, which, for brevity, we shall call curvature effects including long-wave (CEILW) equations, in the following. We then solve them by means of an implicit finite-difference model. Next we describe the experimental facility and summarize the experiments done, and lastly we compare the experimental data with both the numerical results provided by the equations and the analytical results using a shallow-water theory by Gulli (1975), Germain (1984) and Kabbaj (1985).

2. Curvature effects including long-wave equations

Let us consider the two-dimensional movement of a perfect homogeneous fluid of specific mass ρ, initially at rest in a channel of uneven depth (figure 1). We choose a coordinate system where Ox coincides with the free surface at rest and Oy is positive upward, and define (u, v) as the horizontal and vertical components of the velocity, $\eta\,(x,t)$ as the elevation of the free surface, $\xi(x)$ as the equation of the bottom, t as the time and g as the acceleration of gravity. The continuity and dynamical equations are

$$u_x + v_y = 0 \tag{1a}$$

$$u_t + u\cdot u_x + v\cdot u_y = -\frac{1}{\rho}p_x \tag{1b}$$

$$v_t + u\cdot v_x + v\cdot v_y = -\frac{1}{\rho}p_y - g \tag{1c}$$

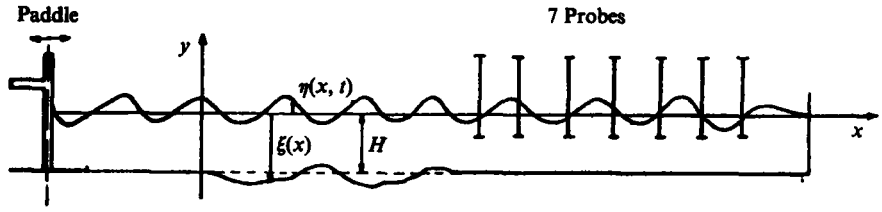

FIGURE 1. Diagram of the experimental installation and notations used.

where $p(x, y, t)$ is the pressure, and the subscripts indicate a derivation with respect to either a space variable or time. The boundary conditions are given by

(*a*) the kinematic condition at the free surface

$$v = \eta_t + u \cdot \eta_x \quad (y = \eta), \tag{2a}$$

(*b*) the dynamic condition at the free surface

$$p = 0 \quad (y = \eta), \tag{2b}$$

(*c*) the impermeability of the bottom

$$v = u \cdot \xi_x \quad (y = \xi). \tag{2c}$$

We non-dimensionalize these equations, using as characteristic length, celerity and pressure the depth in the deep region H, the critical phase speed $C_0 = (gH)^{\frac{1}{2}}$, and the pressure $P_0 = \rho g H$, so that new variables are defined by

$$\alpha = \frac{x}{H}, \quad \beta = \frac{y}{H}, \quad \eta = \frac{\eta}{H}, \quad \xi = \frac{\xi}{H}, \quad u = \frac{x}{C_0}, \quad v = \frac{v}{C_0}, \quad \tau = \left(\frac{g}{H}\right)^{\frac{1}{2}} t, \quad P = \frac{p}{\rho g H}.$$

If we set $p^* = P + \beta$, (1) and (2) become

$$u_\alpha + v_\beta = 0, \tag{3a}$$

$$u_\tau + u u_\alpha + v u_\beta = -p^*_\alpha, \tag{3b}$$

$$v_\tau + u v_\alpha + v v_\beta = -p^*_\beta; \tag{3c}$$

$$v = \eta_\tau + u \eta_\alpha \quad (\beta = \eta) \tag{4a}$$

$$p^* = \eta \quad (\beta = \eta) \tag{4b}$$

$$v - u \xi_\alpha = 0 \quad (\beta = \xi). \tag{4c}$$

Let us assume that the vertical movement of a particle is small compared with the horizontal movement, that is, we use the shallow-water hypothesis, so that we can write $u = u(\alpha, \tau)$; then combining (3*a*) and (4*c*) leads to

$$v = -(\beta - \xi) u_\alpha + u \xi_\alpha, \tag{5}$$

so that

$$v_\tau = -(\beta - \xi) u_{\alpha\tau} + u_\tau \xi_\alpha, \tag{6}$$

$$u v_\alpha = 2 u u_\alpha \xi_\alpha - (\beta - \xi) u u_{\alpha\alpha} + u^2 \xi_{\alpha\alpha}, \tag{7}$$

$$v v_\beta = (\beta - \xi) u_\alpha^2 - u u_\alpha \xi_\alpha. \tag{8}$$

Evaluation of (5) at $\beta = \eta$ combined with the kinematic free-surface boundary condition (4a) leads to the equation

$$\eta_\tau + [u(\eta-\xi)]_\alpha = 0, \tag{9}$$

and (3c) together with (6), (7) and (8) yields

$$p^*_\beta = -(\beta-\xi)[u^2_\alpha - uu_{\alpha\alpha} - u_{\alpha\tau}] + \xi_\alpha[u_\tau + uu_\alpha] - u^2\xi_{\alpha\alpha}, \tag{10}$$

so that, using (4b),

$$p^* = \tfrac{1}{2}[(\eta-\xi)^2 - (\beta-\xi)^2]\,G + (\eta-\beta)\,F + \eta, \tag{11}$$

where

$$G = u^2_\alpha - uu_{\alpha\alpha} - u_{\alpha\alpha},$$

$$F = \xi_\alpha(u_\tau + uu_\alpha) + u^2\xi_{\alpha\alpha}.$$

In the same fashion, the integration of (3b) between the bottom and the free surface, together with (11), leads to

$$(\eta-\xi)(u_\tau + uu_\alpha) + [\tfrac{1}{3}(\eta-\xi)^3 G + \tfrac{1}{2}(\eta-\xi)^2 F + \tfrac{1}{2}(\eta-\xi)^2]_\alpha = -(\eta-\xi)\,\xi_\alpha[\tfrac{1}{2}(\eta-\xi)\,G + F + 1]. \tag{12}$$

Let us now go back to the dimensional variables, and upon noting that $h = \eta - \xi$, from (9) and (12) we get

$$h_t + (hu)_x = 0, \tag{13a}$$

$$h(u_t + uu_x) + [h^2(\tfrac{1}{2}g + \tfrac{1}{2}\phi + \tfrac{1}{3}\Gamma)]_x = -h\xi_x(g + \phi + \tfrac{1}{2}\Gamma), \tag{13b}$$

$$\phi = \xi_x(u_t + uu_x) + u^2\xi_{xx}, \tag{13c}$$

$$\Gamma = h(u^2_x - uu_{xx} - u_{xt}), \tag{13d}$$

where u, v, ξ are here dimensional variables. As can be seen from (5), the vertical component of the acceleration of the particles at the free surface is given by $(\Gamma + \phi)$. So one can say that (13) describes both the slow evolution of a wave over a horizontal bottom and the splitting of an incident wave into transmitted and reflected waves over a submerged obstacle or a change of depth. In other words, (13) describes the propagation of long waves while integrating wave curvature and topographical effects, and so can model the phenomena occurring during either the passage over an obstacle or the reflection of a solitary wave from a vertical wall, where the vertical acceleration of the free surface does seem to have a large influence (Maxworthy 1976; Renouard *et al.* 1985). Now if the bottom is horizontal ($\xi = -H$), then $\xi_x = \xi_{xx} \equiv 0$, so that (13) becomes

$$h_t + (hu)_x = 0, \tag{14a}$$

$$u_t + uu_x + gh_x + \tfrac{2}{3}h_x\Gamma + \tfrac{1}{3}h\Gamma_x = 0, \tag{14b}$$

$$\Gamma = h(u^2_x - uu_{xx} - u_{xt}), \tag{14c}$$

which is the system of equations first obtained by Serre (1953) and later by Su & Gardner (1969). When $\Gamma = 0$, (14) is identical with the Saint-Venant equations or finite-amplitude shallow-water equations. Let us note that (14) (with $\Gamma \neq 0$) has as a particular solution the solitary wave described by

$$\eta = A\,\mathrm{sech}^2\left[\frac{K}{H}(x - ct + x_0)\right], \tag{15}$$

$$u = \frac{c\eta}{H+\eta}, \tag{16}$$

with $K = [3A/4H(1+A/H)]^{\frac{1}{2}}$, and $c = [gH(1+A/H)]^{\frac{1}{2}}$. Such expressions will be adopted to characterize the incident wave in our work. To study the phenomena linked with the reflection of a solitary wave from a plane vertical wall, Mirie & Su (1983) used the same equations as (14), and adopted an implicit finite-difference model to solve them numerically. The numerical model that we used is inspired by them, but improved and modified in such a way that it can take into account an uneven bottom.

3. Laboratory experiments

3.1. *Experimental facility*

In order to study gravity waves, the Institut de Mécanique de Grenoble has some large channels, the largest, used for these experiments, being 36 m long, 0.55 m wide and 1.30 m deep. It is built entirely with glass panels so that there is excellent visualization of the phenomena occurring within it. It is equipped with a piston-type wave paddle, moved with a variable-speed motor. An electromagnetic clutch allows rapid starting and stopping of the paddle, while a crank-arm system, of adjustable eccentricity, allows the variation of the stroke of the piston. The amplitude of the paddle movement ($2e$) can be set between 15.6 and 40 cm, and the period of the movement T between 0.5 and 5 s. A paddle displacement in the positive (downstream) direction generates one or many solitary waves followed by a dispersive tail; a paddle displacement in the opposite direction will generate a dispersive wave. For the present study we need to have only one solitary wave of a given amplitude A, or rather of a given ratio A/H, at a certain distance from the paddle, say at some distance from the shelf or the obstacle. Previous experiments showed that, for a given depth H it is possible to choose values of $2e$ and T to obtain these conditions with great accuracy (Renouard *et al.* 1985).

For the present study we set in the channel either a triangular obstacle, 14.1 cm wide at the bottom and 10 cm in height, or a shelf, 18 m long and 10 cm high. The wave generator was originally conceived to generate periodic sinusoidal waves and hence the paddle motion is not optimum for the study of solitary waves since it will always generate a tail with the desired solitary wave.

In order to avoid any interaction between the solitary wave reflected from the shelf or the barrier and the incident tail, we placed a gate in the zone where the incident solitary wave is clearly separated from the tail for all experimental conditions, i.e. 14 m from the paddle, and quickly dropped it after the incident wave had passed through. In this way the incident wave, and the waves created by its passage over the obstacle were the only phenomena occurring in the downstream part of the channel. The disturbances produced by the dropping of the gate were of much smaller amplitude than the solitary wave or even the tail. They propagated at most with the linear phase speed and were virtually unnoticeable for most experiments. Because of this, the useful length of the channel was reduced to 22 m, which created some difficulties discussed below.

The paddle movements were measured using a linear displacement recorder. The variation in height of the free surface with time at a given point was recorded by seven resistivimetric probes. The precision of each of these probes was about 0.1 mm. One of them, placed immediately upstream of the gate, allowed the determination of the correct time for dropping the gate after the incident solitary wave had completely passed by. The others were situated at various locations in the downstream part of the channel. The origin of the downstream coordinate was chosen either above the centre of the obstacle or above the start of the step. The incident wave

Exp.	H (cm)	A_i (cm)	A_{t1} (cm)	A_{t2} (cm)	A_{t3} (cm)	A_{t4} (cm)
1	30.0	4.25	4.95	0.82	—	—
2	30.0	6.80	8.50	1.61	—	—
3	30.0	7.10	8.85	1.74	—	—
4	30.0	7.50	9.71	1.80	—	—
5	30.0	7.50	9.68	1.82	—	—
6	30.0	9.70	12.90	2.38	—	—
7	25.0	1.78	2.22	0.70	—	—
8	25.0	2.57	3.14	0.75	—	—
9	25.0	3.84	4.74	1.16	—	—
10	25.0	5.75	7.94	2.03	—	—
11	25.0	7.17	10.34	2.47	—	—
12	25.0	7.40	10.63	2.47	—	—
13	22.2	2.07	2.75	0.88	—	—
14	22.2	2.73	3.68	1.07	—	—
15	22.2	3.65	4.93	1.41	—	—
16	22.2	4.17	5.91	1.70	—	—
17	22.2	4.61	6.48	1.88	—	—
18	22.2	5.16	7.48	2.20	—	—
19	22.2	5.62	8.10	2.29	—	—
20	20.0	1.63	2.38	0.98	0.44	—
21	20.0	2.08	3.08	1.09	0.28	—
22	20.0	2.43	3.56	1.21	0.20	—
23	20.0	2.93	4.30	1.56	0.34	—
24	20.0	3.65	5.31	1.80	0.33	—
25	20.0	3.90	5.73	2.06	0.51	—
26	20.0	4.36	6.78	2.29	0.52	—
27	18.1	1.59	2.38	1.11	0.52	—
28	18.1	2.07	3.27	1.37	0.43	—
29	18.1	2.39	3.67	1.50	0.56	—
30	18.1	2.69	4.07	1.79	0.70	—
31	18.1	2.90	4.49	1.92	0.68	—
32	15.0	1.62	Break	1.72	0.86	0.44
33	15.0	2.18	Break	2.18	1.10	0.56

TABLE 1. Experimental results for the passing of a solitary wave over a shelf. H, depth in front of the shelf; A_i, amplitude of the incident wave; A_{tj}, amplitude of the jth transmitted wave; A_r, amplitude of the reflected wave. All amplitudes and depths are in cm.

was measured at $X = -15H$ before the barrier and at $X = -3.0$ m before the shelf. We performed a total of 80 experiments which are listed in tables 1 and 2, where we indicate the depth in front of the obstacle H, the amplitudes of the incident wave A_i, the reflected wave A_r, and transmitted waves A_{tj} (here the subscript j denotes the jth transmitted wave).

3.2. *Study of wave propagation over a step* (*table* 1)

One incident solitary wave will evolve into at least two solitary waves ranked in order of decreasing amplitude and followed by a small dispersive tail. During this fission process there are often noticeable changes of amplitude, so that the measurement of this phenomenon is somewhat tricky. On the one hand, the amplitude of a transmitted wave must not be measured before the wave-sorting process is completed. But on the other hand, if the distance between the beginning of the step and the point of measurement is too large, viscous damping may be appreciable. Therefore, from all the available data records above the step, the amplitude of each transmitted

Exp.	H (cm)	A_i (cm)	A_r (cm)	Exp.	H (cm)	A_i (cm)	A_t (cm)	A_r (cm)
34	20.0	2.87	0.59	58	13.3	3.89	0.84	—
35	20.0	3.40	0.63	59	13.3	5.89	1.20	—
36	20.0	3.65	0.68	60	12.5	3.20	0.88	—
37	20.0	3.92	0.63	61	12.5	4.08	1.07	—
38	20.0	3.94	0.65	62	12.5	4.87	1.18	—
39	20.0	5.07	0.68	63	25.0	5.10	4.80	—
40	20.0	5.78	0.72	64	25.0	7.40	6.90	—
41	20.0	6.45	0.92	65	25.0	10.00	9.30	—
42	20.0	7.74	0.91	66	25.0	12.20	11.30	—
43	18.1	2.60	0.52	67	20.0	4.20	3.86	—
44	18.1	2.90	0.59	68	20.0	5.86	5.46	—
45	18.1	5.30	0.71	69	20.0	8.00	7.38	—
46	18.1	6.26	0.85	70	20.0	9.90	9.10	—
47	18.1	7.20	0.88	71	20.0	11.90	10.80	—
48	16.0	2.65	0.62	72	15.0	2.96	2.60	0.41
49	16.0	4.03	0.69	73	15.0	4.35	3.80	0.60
50	16.0	5.92	0.91	74	15.0	5.81	5.00	0.65
51	16.0	7.00	1.04	75	15.0	6.56	5.60	0.80
52	15.0	2.34	0.63	76	15.0	8.40	7.31	1.20
53	15.0	3.86	0.70	77	12.5	2.50	1.95	0.60
54	15.0	5.06	0.94	78	12.5	4.75	3.70	0.80
55	15.0	5.09	0.96	79	12.5	6.00	4.85	0.95
56	15.0	6.49	1.09	80	12.5	6.30	5.10	1.05
57	13.3	2.67	0.76					

TABLE 2. Experimental results for the passing of a solitary wave over an obstacle. H, depth in front of and behind the obstacle; A_i, amplitude of the incident wave; A_t, amplitude of the transmitted wave; A_r, amplitude of the reflected wave. All amplitudes and depths are in cm.

solitary wave was measured on the record showing a fully separated solitary wave, which was the closest to the origin of the abscissa. Since for other experimental conditions a length of about 15 m was required for such a wave-sorting process, the whole length (18 m) was necessary for the complete study of the transmitted waves. But that left only 4 m between the gate and the step to study the reflected wave. Hence we were obliged to do two different sets of experiments: one for the study of the transmitted waves, for which the whole length of the step was needed; and one for which the step length was reduced to 6 m, in order to facilitate measurement of the reflected wave.

However, with regard to the amplitudes and the depth, the constraints were different for each of these studies. For the study of transmitted waves, the depth was chosen between 15 and 30 cm. For depths equal to or smaller than 15 cm, even the smallest waves generated by the paddle experienced breaking above the step. For depths larger than 30 cm, the sorting distance for the transmitted wave is longer than the available length of the step (18 m). The amplitude of the incident solitary wave was chosen so as to avoid breaking of the first transmitted wave over the shelf. Probes were situated every 3 m between $X = -3.0$ m and $X = 15.0$ m. For the study of reflected waves, the depth was chosen between 12.5 and 20.0 cm. The upper limit was adopted in order to secure a good relative precision for the measurements, since the relative height of the step and the amplitude of the reflected waves vary proportionally. The lower limit was fixed by the appearance of vortices in the fluid near the step when the total depth approaches the step height. The reflected-wave amplitude

was measured at the location where it appeared well separated from the incident wave, and which was the closest to the origin of the step to minimize the influence of viscous effects. For that purpose the probes were situated every other 3 m between $X = -15$ m and $X = +3$ m.

3.3. *Study of wave propagation over an isolated obstacle* (*table* 2)

When the obstacle height H_s became important *vis-à-vis* the total depth, i.e. $H_s/H = O(1)$, a vortex appeared in the fluid immediately downstream of the obstacle, mainly when the amplitude of the incident wave was large. Such a vortex absorbs a large part of the available energy, and we verified that it affects the amplitude of the transmitted wave. The generation of such a vortex is not represented by the theoretical or numerical model of concern here, and we shall ignore it. It was easier to obtain experimental conditions that avoided such a vortex than those reported in §3.2. The transmitted wave essentially retained the amplitude of the incident wave, and recovered an equilibrium profile only a short distance downstream of the obstacle. In most of our experiments, the barrier was only a source of limited disturbances which did not appear to affect the evolution of the wave. None the less, a closer look revealed the existence of a reflected solitary wave, the amplitude of which increased with the relative height of the obstacle. For incident waves of an amplitude comparable with the obstacle height, even for incident waves of very large amplitude, we never noticed a breaking of the wave over or after the barrier. We limited our study to depths smaller than 25 cm, since as soon as the depth over the barrier was larger than 15 cm no reflected solitary wave was observed; this is explained by the fact that their amplitude would have been of the order of the amplitude of the dispersive waves generated by propagation over the barrier. The lower limit for the depth was 12.5 cm, since for smaller values a vortex appeared as noted above. The normalized amplitude of the incident wave for these experiments was kept in the range $0.2 < A_i/H < 0.6$.

4. Comparison between experimental results and first-order shallow-water theory

In Germain (1971*a*, *b*; 1972) the basic hypotheses of a generalized shallow-water theory are explained. Such a generalization allows one to describe phenomena occurring at the start of a paddle movement or around obstacles, and over bottom topographies. This theory was applied to a solitary wave propagating over a barrier by Gulli (1975) and to a solitary wave propagating on to a shelf by Kabbaj (1985). They obtained analytical expressions characterizing the transmitted and reflected waves generated by an incident solitary wave.

4.1. *Solitary wave passing over a step*

Germain (1984) and Kabbaj (1985) provide the number n of transmitted waves as well as their amplitudes A_{tj} in terms of the amplitude of the incident wave A_i, the depth of the deep water H and the depth over the step H_1. In our notation the results are

(i) for the transmitted waves

$$\frac{A_{tj}}{A_i} = \frac{H_1}{H}(M-j)^2, \tag{17}$$

$$M = \frac{1}{2}\left\{\left[1+\frac{16(H/H_1)^{\frac{5}{2}}}{1+(H/H_1)^{\frac{1}{2}}}\right]^{\frac{1}{2}}-1\right\}$$

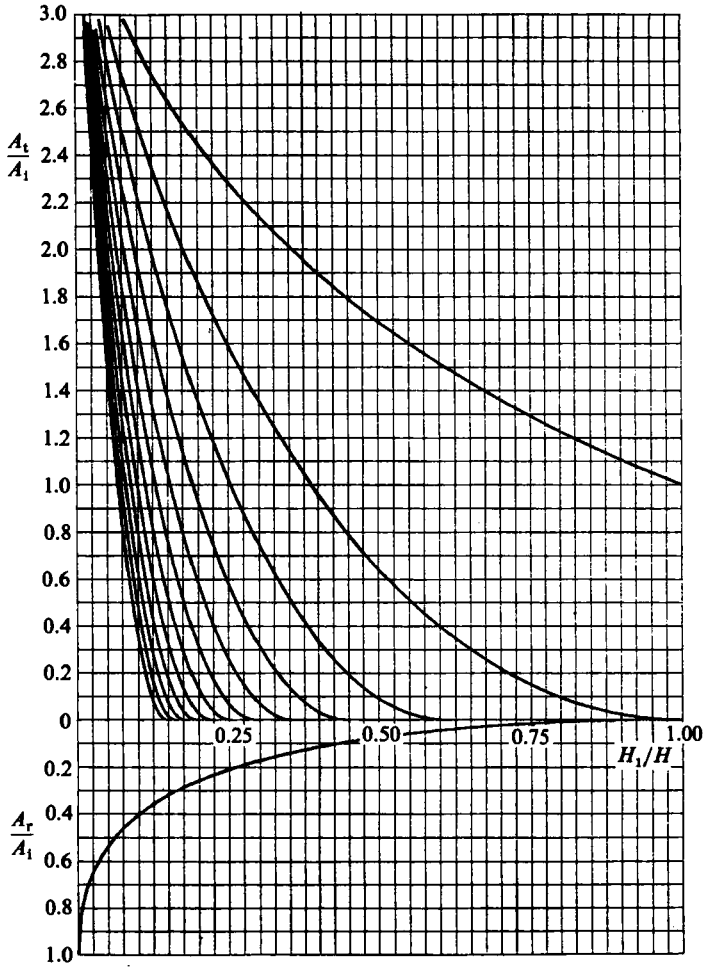

FIGURE 2. Passing of a solitary wave over a step: number and amplitudes of the transmitted waves (A_t/A_i, upper part) and reflected waves (A_r/A_i, lower part) with respect to the depth ratio (H_1/H).

with the number of transmitted waves being

$$n = [M] \quad \text{(largest integer} \leqslant M);$$

(ii) for the reflected wave

$$\frac{A_r}{A_i} = \frac{1}{4}\left\{\left[\frac{9-7(H_1/H)^{\frac{1}{2}}}{1+(H_1/H)^{\frac{1}{2}}}\right]^{\frac{1}{2}} - 1\right\}^2. \tag{18}$$

Figure 2 expresses these results graphically: the abscissa is the ratio H_1/H of the depth H_1 over and H in front of the step. The upper part of the figure gives the ratios of the amplitude of the first twelve transmitted waves with respect to the amplitude of the incident wave (A_{tj}/A_i), while the lower part gives the ratio of the amplitude of the reflected wave relative to the amplitude of the incident wave (A_r/A_i).

These theoretical results are supported by our experimental results, and we have verified that the number and amplitudes of transmitted waves increase with the relative height of the step, with similar results for the reflected wave. We also verified that there are always at least two transmitted waves and only one reflected wave, and that the amplitude of the second transmitted wave can be very small if the

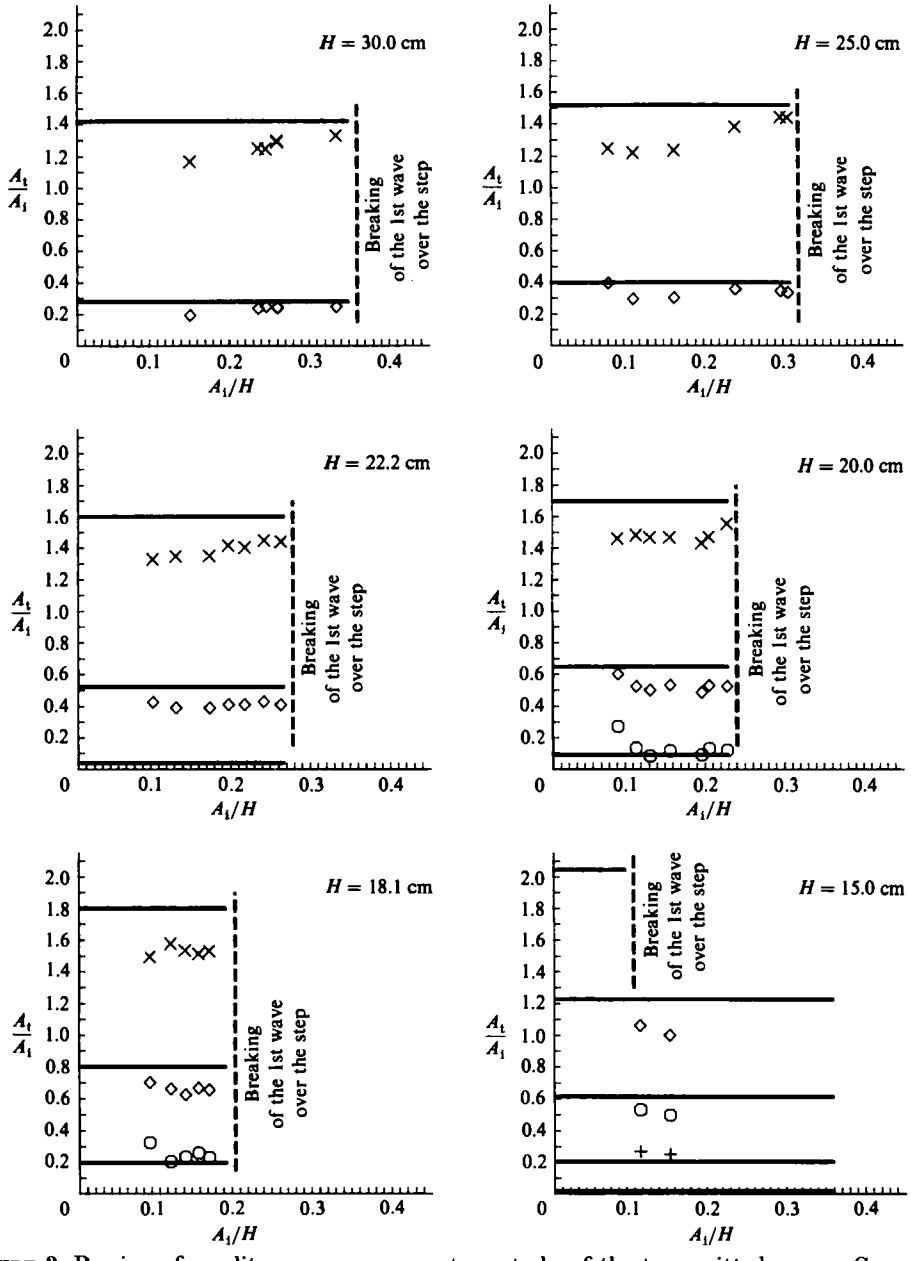

FIGURE 3. Passing of a solitary wave over a step: study of the transmitted waves. Comparison between the shallow-water theory results (solid horizontal lines) and the measured first (×), second (◇), third (○) and fourth (+) transmitted solitary waves.

relative height of the step is also small, i.e. $H_1/H = O(1)$. Moreover, such results allow an understanding of the experimental difficulties described in the previous section.

A comparison between the experimental data is given both for the transmitted (figure 3) and for the reflected (figure 4) waves. In figure 3 the dashed vertical lines indicate the upper limit for A_i/H above which the first transmitted wave breaks. In both figures one can see that the ratios of the amplitudes A_t/A_i or A_r/A_i are practically independent of the normalized amplitude of the incident wave (A_i/H),

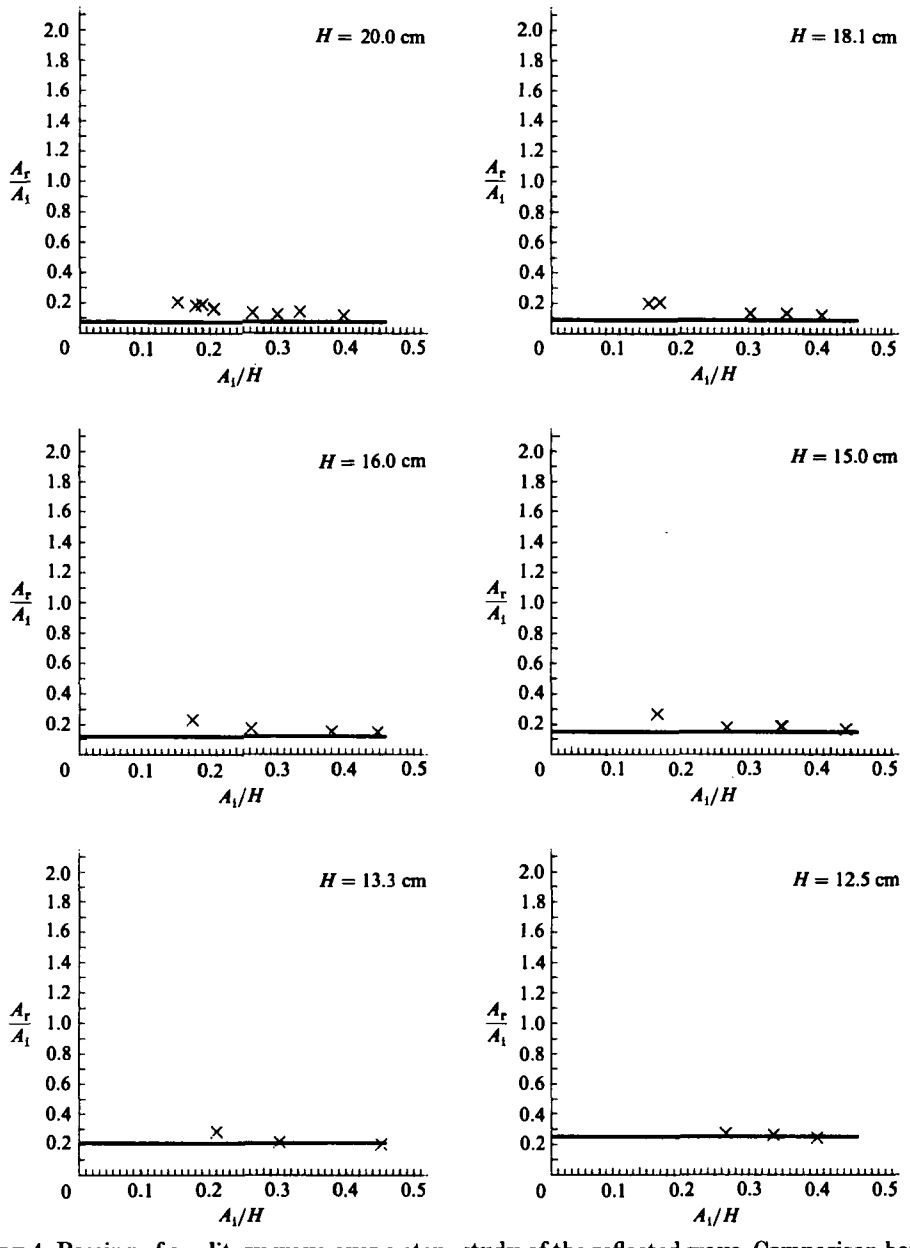

FIGURE 4. Passing of a solitary wave over a step: study of the reflected wave. Comparison between the shallow-water theory results (solid horizontal lines) and the measured reflected wave (×).

as predicted, and are in good agreement with the theoretical values. The slight dependence of A_t/A_i on A_i/H, apparent mainly on the first transmitted wave, can be explained as follows.

The solitary waves of higher relative amplitude also have a smaller characteristic wavelength and hence their fission over the shelf is completed at a shorter distance from the step. Therefore the amplitude measurement must be performed closer to the step in order to avoid most of the viscous damping effects. Concerning the reflected wave, the slight decrease of A_r/A_i with increasing A_i/H, which can be

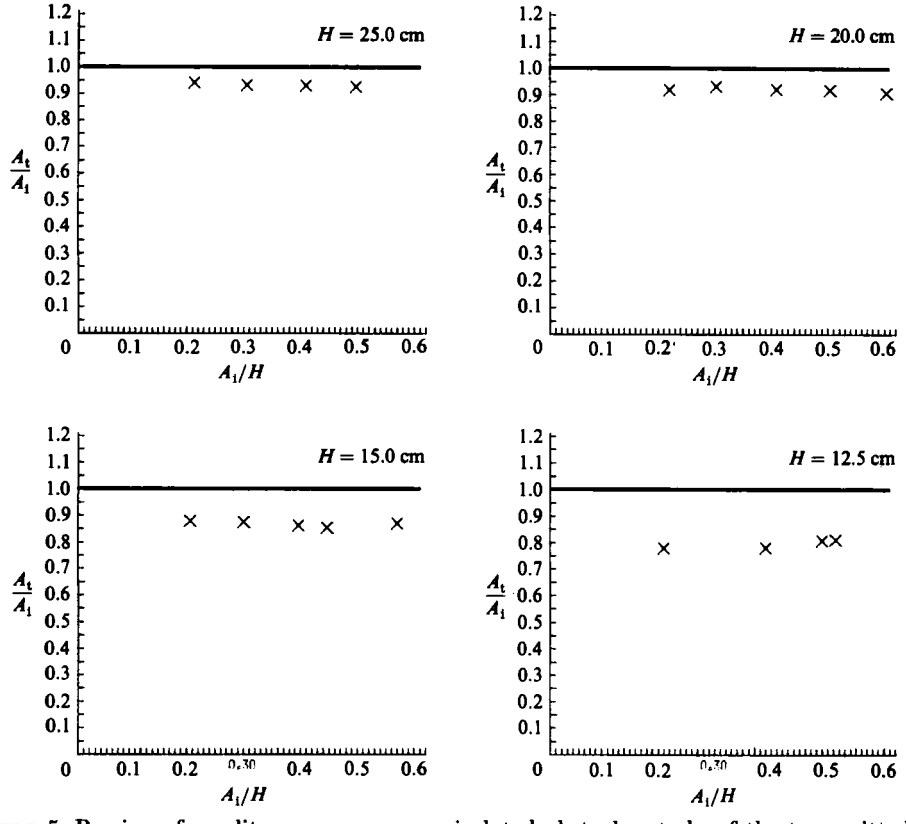

FIGURE 5. Passing of a solitary wave over an isolated obstacle: study of the transmitted wave. Comparison between the shallow-water theory result (solid horizontal line = amplitude of incident wave) and the measured transmitted wave (×).

observed in figure 4, may be linked with the loss of energy due to vortices observed near the step when A_i/H becomes important and tends to be stronger when A_i/H or H_s increases. One should note (figure 4) that, although the relative errors seem large, in fact, in absolute value they are of the same order of magnitude as the errors observed for transmitted waves. It is also of interest to note that the observed transmitted amplitudes are always smaller than the predicted transmitted amplitudes, but that the observed reflected amplitudes are always larger than the predicted reflected amplitudes. Although we have no justification for this, we suggest that it might be because the theory is limited to the first-order approximation, which might transfer too much energy to the transmitted wave. Perhaps higher-order developments would show a behaviour closer to the experimental results.

4.2. *Solitary wave passing over an obstacle*

The analytical results at the first order of approximation obtained by Gulli (1975) are very simple: there is always only one transmitted wave whose amplitude is equal to the incident-wave amplitude, and no reflected wave. As a first approximation and for most practical purposes, it is what we observed experimentally. Only one solitary wave is recorded downstream of the obstacle, and its amplitude is of the same order of magnitude as the amplitude of the incident wave (figure 5). None the less, for $H > 15$ cm ($H_s < \frac{2}{3}H$) the reflected wave is absolutely negligible. For $H \leqslant 15$ cm such

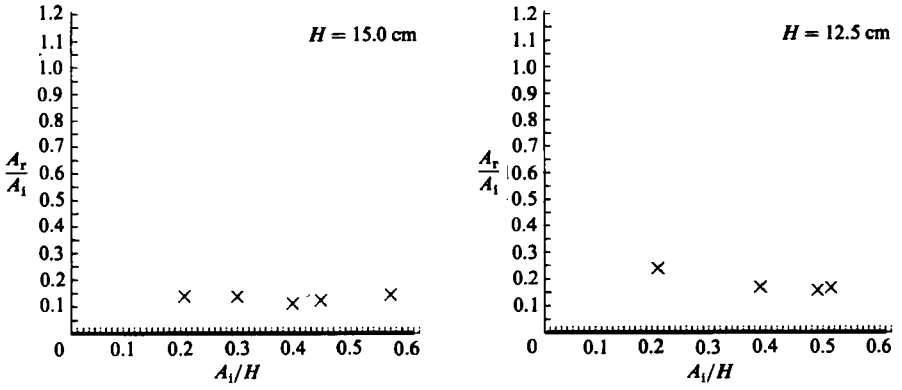

FIGURE 6. Passing of a solitary wave over an isolated obstacle: study of the reflected wave. Comparison between the shallow water-theory result (solid horizontal line coinciding with the abscissa axis) and the measured reflected wave (×).

a wave is observable, though of very small amplitude (figure 6). The appearance of such a reflected wave and the slight decrease of the transmitted-wave amplitude can be interpreted as higher-order effects, which have been neglected at the first order of approximation. Moreover, for the smaller depths, the vortex appearing after the obstacle is significant, and we observed that the decrease of the transmitted-wave amplitude was larger when this vortex appears. This would explain why the best result, when comparing experiments with this theory, were obtained when the depth was larger (H_s/H small).

5. Comparison between experimental results and numerical results from the CEILW equations

As previously mentioned, we adopted an implicit finite-difference model to solve the CEILW equations when the bottom was uneven. If tested successfully against the experimental data, such a model could then be extended to study the effects of a continental shelf or a submerged obstacle on the propagation of an incident wave in the ocean, and its effect on the thermocline level.

5.1. *Solitary wave passing over a step*

Let us consider one particular experiment when the depth H was 20 cm, the step had a height of 10 cm, and an incident solitary wave of amplitude $A_i = 3.65$ cm was recorded at $X = -3$ m in front of the step. The numerical computation started ($t = 0$) when the crest of the incident wave was at $X = -3$ m. The shape of this wave as well as the velocity distributions are given by (15) and (16) respectively. Figure 7 shows the shape of the free surface between times $t = 0$ and 10.74 s. The vertical dashed lines with arrows indicate the positions of the recorders. We were obliged to introduce a distortion in our model, since a first computation, with a change of depth within one space-step of the grid of discretization ($x = 6$ cm) leads to high-frequency numerical disturbances at the free surface around $X = 0$. So we joined the two regions of different depths by a half-sinusoidal profile step stretched to 60 cm. Within the range of validity of the first-order shallow-water theory such a step profile distortion is legitimate. Since the equations used in the model in fact integrate third-order terms, one can expect slight differences between numerical and experimental results, and the experiments will show some discrepancies.

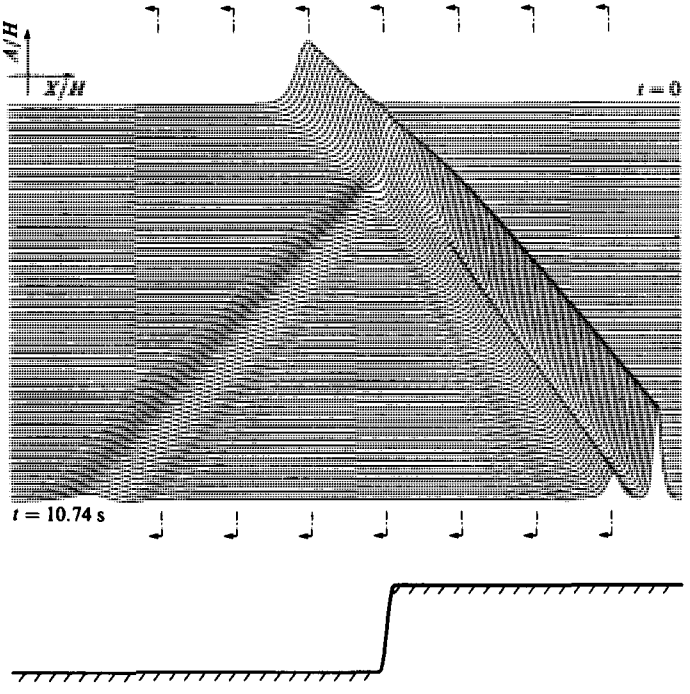

FIGURE 7. Passing of a solitary wave over a step. Numerical study of the shape of the free surface between times $t = 0$ and 10.74 s. $A_1 = 3.65$ cm; $H = 20$ cm; $H_s = 10$ cm. The vertical dashed lines indicate the positions of the recorders for comparison with figure 8.

We can see (figure 7) that the incident solitary wave first grows in amplitude, then broadens and decreases in amplitude before splitting into two transmitted waves followed by a small train of dispersive waves. A reflected wave again followed by a tiny dispersive wave was also generated. Such a result is in perfect agreement with the analytical predictions of Germain (1984), but moreover provides us with the shape of the free surface at each time and a more accurate description, since the equations represent the phenomena to the third-order of approximations in (A_1/H). This is illustrated by comparing the experimental data and the computed results at the various locations (figure 8). Let us recall that the computations start ($t = 0$) when the crest of the incident wave is at $X/H = -15$ in this example; hence the upper figures ($X/H = -45, -30, -15$) show the reflected wave, and the lower figures show the incident and transmitted waves. The time is positive leftward in this figure as well as in figure 10. We can verify that, beside a slight phase shift and a small difference in amplitude, the recorded and numerical curves are practically identical. But the experiments show the existence of a third transmitted wave of very small amplitude, also predicted by Germain (1984) as one can check on figure 2 with $H_1/H = 0.5$, and this does not appear in the computations. Very likely the distortion introduced in the shape of the step in the numerical model is responsible for this slight disagreement. Many other comparisons between experimental data and numerical results show the same good agreement, and thus enable us to affirm that our model of the CEILW equations allows a practical way of computing the shape of the free surface as well as the velocity distributions each time an incident solitary wave passes over a shelf.

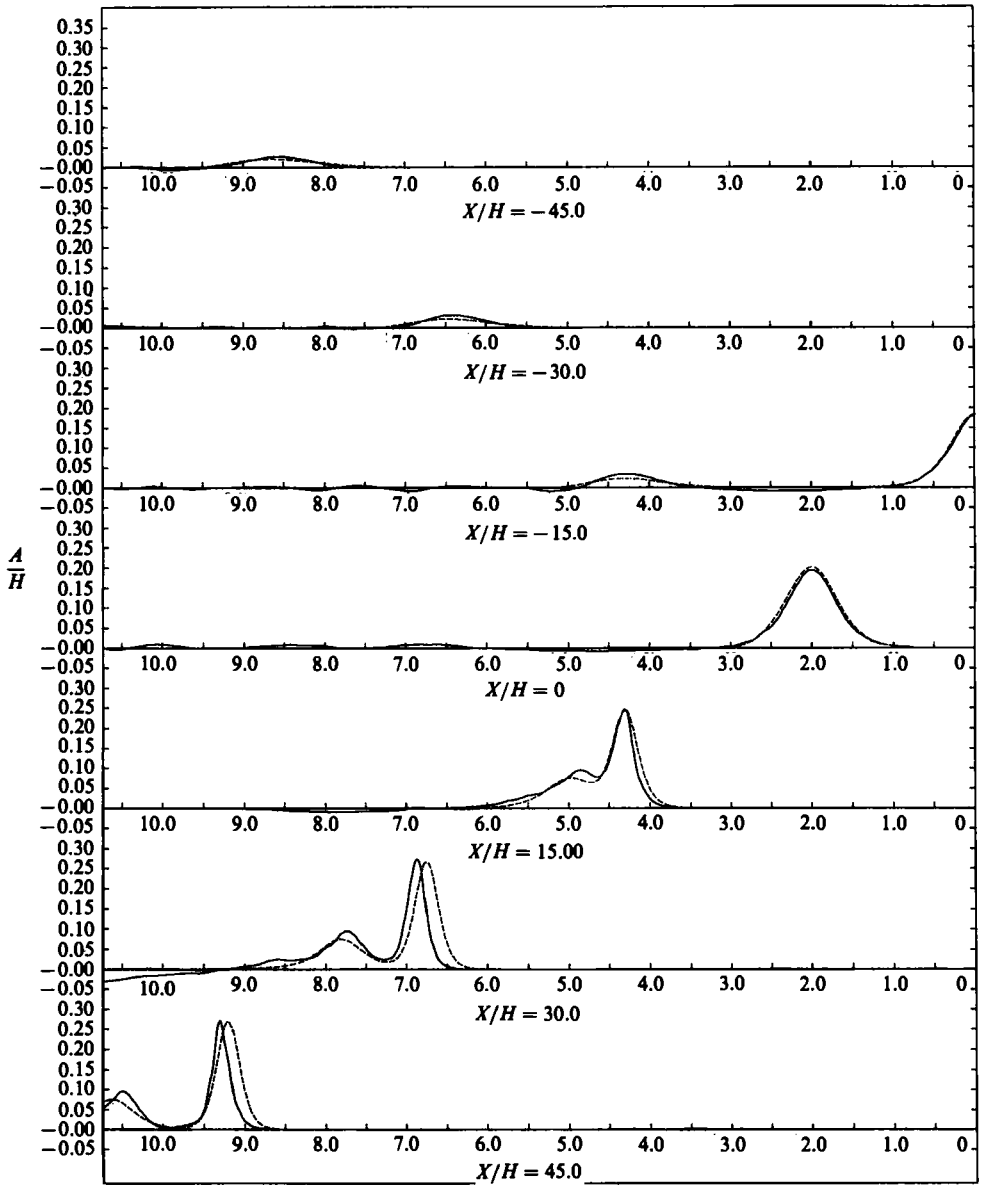

FIGURE 8. Passing of a solitary wave over a step. Comparison between the computed (dashed lines) and recorded (solid lines) surelevations of the free surface of various locations before and after the step (see figure 7 for experimental conditions and probes' location).

5.2. *Solitary wave over an obstacle*

The qualitative agreement noted above also holds true when we compare the experimental data with the computations analysing solitary-wave evolution over an obstacle. Here again, for computational purposes it was necessary to choose a smoother shape than the triangular obstacle actually used in the experiments. The numerical scheme was very sensitive to abrupt changes of bottom slope, hence a sinusoidal profile was used to approximate the triangular obstacle. Nevertheless, such a modification proved to introduce no major disagreement with the observations,

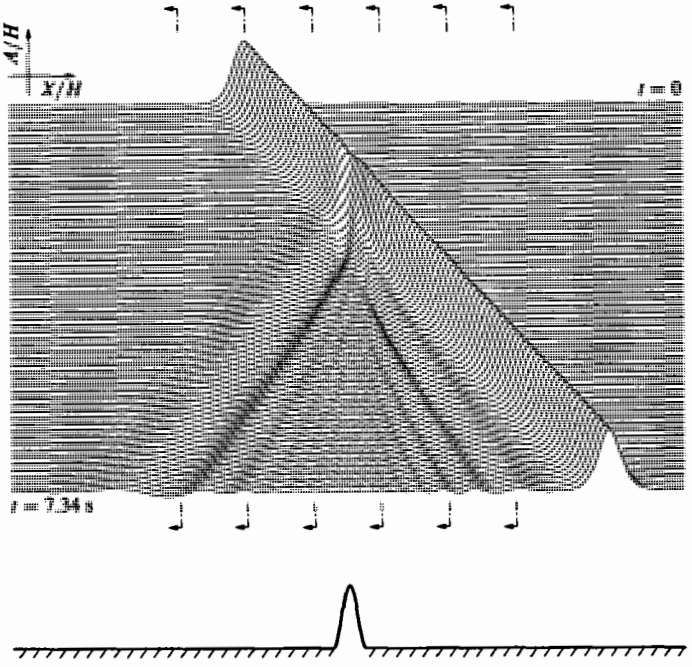

FIGURE 9. Passing of a solitary wave over an isolated obstacle. Numerical study of the shape of the free surface between times $t = 0$ and 7.34 s. $A_1 = 10.0$ cm; $H = 25$ cm; $H_s = 10$ cm. The vertical dashed lines indicate the positions of the recorders for comparison with figure 10.

thus confirming the validity of the shallow-water hypothesis in the study of such phenomena.

Figure 9 shows the computed shape of the free surface at various times between $t = 0$ ($X/H = -15$) and $t = 7.34$ s. Gulli (1975) predicted a transmitted wave equal to the incident wave, and no reflected wave. The computations, in agreement with the experimental data, show that there was a slight change of amplitude of the transmitted wave which was accompanied by a train of dispersive waves, and a small but noticeable reflected solitary wave also accompanied by dispersive waves.

Figure 10 provides a direct comparison between the experimental and numerical data, and one can note the very good agreement between them.

Thus these experiments, while plainly supporting the analytical results given by Germain (1984) in the framework of the shallow-water theory, allow us to verify the accuracy of a numerical model using the CEILW equations. The ability of such a set of equations to describe the phenomena involved in the propagation of a solitary wave over a step or an isolated obstacle is illustrated here. It is anticipated, therefore, that the CEILW equations will provide a better description of the influence of isolated or semi-infinite bottom topography on the evolution of solitary waves in the vicinity of a continental shelf. They could also be extended to describe the generation of internal solitary waves by baroclinic incident waves passing on to a shelf (cf. Djordjevic & Redekopp 1978).

The authors wish to express their gratitude to Professor J. P. Germain for the many fruitful discussions and suggestions. The experiments have been carried out with the valuable help of Michael and Stanislas Kwiatkowski and P. Licari.

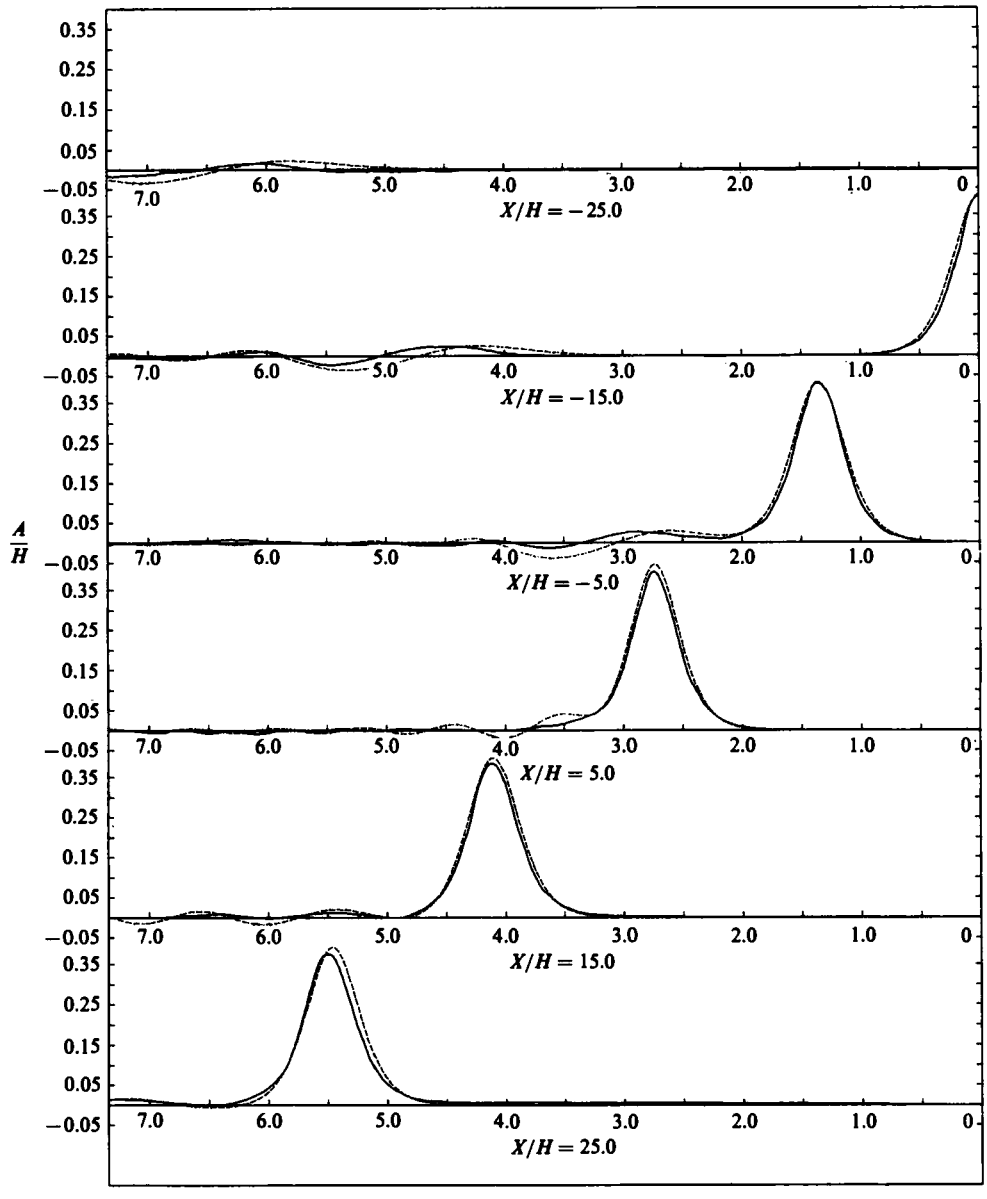

FIGURE 10. Passing of a solitary wave over an isolated obstacle. Comparison between the computed (dashed lines) and recorded (solid lines) surelevations of the free surface at various locations before and after the obstacle (see figure 9 for experimental conditions and probes' locations).

REFERENCES

DJORDJEVIC, V. D. & REDEKOPP, L. G. 1978 The fission and disintegration of internal solitary waves moving over two-dimensional topography. *J. Phys. Oceanogr.* **8**, 1016–1024.

FENTON, J. D. & RIENECKER, M. M. 1982 A Fourier method for solving nonlinear water-wave problems: application to solitary-wave interactions. *J. Fluid Mech.* **118**, 411–443.

GERMAIN, J. P. 1971*a* Sur une généralisation de la théorie des mouvements en eau peu profonde. *C. R. Acad. Sci. Paris* **273A**, 1093–1096.

GERMAIN, J. P. 1971*b* Sur le caractère limité de la théorie des mouvements des liquides parfaits en eau peu profonde. *C. R. Acad. Sci. Paris* **273A**, 1171–1174.

GERMAIN, J. P. 1972 Théorie générale des mouvements d'un fluide parfait pesant en eau peu profonde de profondeur constante. *C. R. Acad. Sci. Paris* **274A**, 997–1000.

GERMAIN, J. P. 1984 Coefficients de réflexion et de transmission en eau peu profonde. *Instytut Budownictwa Wodnego, Gdansk, Rozprawy Hydzotechniezne, Rep. No.* 46.

GORING, D. C. 1978 Tsunamis – the propagation of long waves onto a shelf. *California Institute of Technology, Pasadena, Rep. KHR*-38.

GULLI, L. 1975 Etude du passage d'une houle en eau peu profonde sur une barrière verticale immergée. Thèse, Université Scientifique et Médicale de Grenoble.

KABBAJ, A. 1985 Contribution à l'étude du passage des ondes de gravité et de la génération des ondes internes sur un talus, dans le cadre de la théorie de l'eau peu profonde. Thèse, Université Scientifique et Médicale de Grenoble.

MCCOWAN, J. 1894 On the highest wave of permanent type. *Phil. Mag.* **38**, 351.

MADSEN, O. S. & MEI, C. C. 1969 The transformation of a solitary wave over an uneven bottom. *J. Fluid Mech.* **39**, 781–791.

MAXWORTHY, T. 1976 Experiments on collisions between solitary waves. *J. Fluid Mech.* **76**, 177–185.

MIRIE, R. M. & SU, C. H. 1982 Collisons between two solitary waves. Part 2. A numerical study. *J. Fluid Mech.* **115**, 475–492.

RENOUARD, D., SEABRA-SANTOS, F. J. & TEMPERVILLE, A. 1985 Theoretical and experimental studies of the generation, damping and reflexion of a solitary wave. *Dyn. Atmos. Ocean* **9**, 341–358.

SEABRA-SANTOS, F. J. 1985 Génération, propagation et réflexion des ondes solitaires. Thèse, Université Scientifique et Médicale de Grenoble.

SERRE, F. 1953 Contribution à l'étude des écoulements permanents et variables dans les canaux. *Houille Blanche*, 374–385.

STREET, R. L., BURGES, S. J. & WHITFORD, P. W. 1968 The behavior of the solitary waves on a stepped slope. *Stanford University Tech. Rep.* 93.

SU, C. H. & GARDNER, C. S. 1969 Korteweg–de Vries equation generalizations. III. Derivation of the Korteweg–de Vries equation and Burgers equations. *J. Math. Phys.* **10**, 536–539.

SU, C. H. & MIRIE, R. M. 1980 On head-on collisions between two solitary waves. *J. Fluid Mech.* **98**, 509–525.